ISSN: 2476-6909; Modares. Mech. Eng. *2025;25(11):717-724.*

Modares Mechanical Engineering

DOI: 10.48311/mme.2025.96909.0
journal homepage: mme.modares.ac.ir

Experimental Assessment of Fracture in Rigid Nanocomposite Foams Weakened by a Pre-Crack in Mixed-Mode I/II

Mohammad Mahdi Touiserkani, Mahdi Heydari-Meybodi*

Department of Mechanical Engineering, Yazd University, Yazd, Iran.

ARTICLE INFO

Article Type
Original Research

Article History
Received: August 01, 2025
Revised: October 31, 2025
Accepted: November 08, 2025
ePublished: November 22, 2025

ABSTRACT

Rigid nanocomposite foams reinforced with nanoclay have low density and high mechanical strength. Additionally, they offer improved thermal and fracture properties, making them attractive for advanced structural applications. This study, examines the effect of nanoclay content (0, 1, 2, and 3 wt%) on the mechanical and fracture behavior of rigid Polyurethane (PUR) foams under mixed-mode I/II loading. The samples are produced using ultrasonic dispersion and subjected to uniaxial tensile and fracture experiments with Asymmetric Edge Notch Disc Bend (AENDB) specimens. Fracture toughness and stress intensity factors are analyzed using Finite Element Modeling (FEM). The results show that adding up to 2 wt% of nanoclay enhances tensile and fracture resistance, while 3 wt% reduces strength due to nanoparticle agglomeration. Significantly, the specimen with 2 wt% of nanoclay shows the best performance, with about 35% increase in tensile strength, 25% in fracture displacement, and up to 32% improvement in fracture load under Mixed-Mode I/II conditions. In contrast, the 3 wt% sample exhibits reductions of about 18% in tensile properties and 16% in mixed-mode fracture load. These findings highlight the importance of optimizing nanoclay concentration to achieve superior fracture performance in rigid PUR foams.

Keywords: Nanocomposite; Nanoclay; PUR Foam; Mixed-Mode I/II Fracture; Finite Element Modeling.

How to cite this article
Touiserkani M.M, Heydari-Meybodi M, Experimental Assessment of Fracture in Rigid Nanocomposite Foams Weakened by a Pre-Crack in Mixed-Mode I/I. Modares Mechanical Engineering; *2025;25(11):717-724.*

*Corresponding author's email: m.heydari.m@yazd.ac.ir
*Corresponding ORCID ID: 0000-0002-0181-7050

1- Introduction

Rigid nanocomposite foams are a class of lightweight materials that consist of a polymer matrix reinforced with nanoscale fillers such as nanoclay, carbon nanotubes, or graphene. These materials inherently reduce density while simultaneously enhancing important mechanical properties including stiffness, tensile strength, and impact resistance [1-5]. The incorporation of nanofillers also improves the functional properties of foams such as thermal insulation, flame retardancy, and dimensional stability, making them more suitable for a variety of demanding environments [6-10].

Among the various types of nanoscale reinforcements, nanoclay has received more attention due to its unique combination of a high aspect ratio, layered silicate morphology, and excellent compatibility with polymer matrices. This compatibility ensures strong interfacial adhesion, which is critical for efficient load transfer and improved mechanical integrity [2, 11-15]. Nanoclay not only hinders crack initiation and propagation within the polymer matrix but also reduces gas permeability and enhances thermal conductivity, contributing to improved overall thermal performance [8, 16, 17]. As a result, the combination of nanoclay with rigid foams can find various applications across diverse engineering sectors because of their outstanding strength-to-weight ratio and multifunctional capabilities. For example, in automotive manufacturing, these materials help reduce the weight, without sacrificing safety or thermal insulation. Similarly, in aerospace, nanocomposite foams contribute to lighter aircraft interiors, leading to improved fuel efficiency [18, 19]. Within the construction industry, these foams serve as energy-efficient insulating cores that also provide necessary structural support [20-22]. With the rising global demand for materials that combine lightweight properties with high strength, increasing attention has been directed toward enhancing the formulation, fabrication techniques, and durability of rigid nanocomposite foams, especially in the context of real-world service conditions [23, 24].

The mechanical response of nanocomposite foams under typical loading scenarios has been explored in earlier research. Previous studies have shown that rigid nanocomposite foams are vulnerable to mechanical and environmental degradation, particularly when subjected to complex loading or multiaxial stress states. Several investigations have examined the effects of nanoparticles on the mechanical behaviour of foams. Significant findings have been reported from these studies (see, for example, Ref. [9, 16, 25-27]). For instance, in Ref. [25], mechanical compression tests revealed that incorporating 5 wt% of organoclay into PUR substantially enhanced its mechanical properties, with a 650% increase in compressive strength and a 780% increase in modulus. Similarly, Saha et al. [17] showed that rigid PUR foams reinforced with 1 wt% of titanium oxide (TiO_2), nanoclay, or carbon nanofibers (CNFs) exhibited improved mechanical and thermal properties, with CNFs providing the greatest enhancement and TiO_2 the least. In addition, Javni et al. [25] found that nano-silica acted as a physical crosslinker in flexible PUR foams, increasing hardness and compressive strength, while micro-silica reduced these properties but improved rebound resilience; moreover, foam density remained largely unchanged up to 20% filler content. Additionally, Kim et al. [28] reported that increasing nanoclay content in rigid PUR foams decreased density and compressive strength but enhanced thermal properties, including elevated glass transition and decomposition temperatures. Maharsia and Jerro [29] investigated nanoclay hybrid syntactic foams. Their results showed enhanced tensile strength and toughness with the incorporation of 2–5% nanoclay. In addition, the presence of nanoclay particles effectively delayed crack initiation and propagation, leading to improved damage tolerance. Besides, in a 2020 study, Zhang et al. [30] developed rigid PUR foams using nano-SiO_2 and biomass fillers (peanut shell, pine bark), evaluating their mechanical and structural performance. All composites met the compressive strength requirements for insulation, with nano-SiO_2 providing higher strength, density, thermal stability, and finer cell structure, while biomass fillers led to lower density and residual content but still maintained acceptable mechanical properties. While numerous studies have addressed the influence of nanoparticles on the overall mechanical properties of polymeric foams, their specific impact on the fracture behavior of pre-cracked foams has been largely overlooked. To the best of the authors' knowledge, Ref. is the only study that specifically addresses this aspect, in which Saha et al. investigated the Mode-I fracture behavior of rigid nanocomposite foams by examining the fracture toughness of neat rigid PUR foam reinforced with various nanoparticles using Single Edge Notched Bending (SENB) specimens under three-point bending conditions. Four types of nanoparticles were evaluated: titanium oxide (5, 10, and 35 nm), nanoclay, carbon nanofibers, and multiwall carbon nanotubes (MWNTs). Among them, the foam containing 0.5 wt% CNFs exhibited the highest improvement in fracture toughness, with an increase of approximately 28% compared to the unreinforced foam.

Given the practical relevance of Mixed-Mode I/II loading in structural applications, where tensile and shear forces act simultaneously, recent studies have increasingly focused on the fracture behavior of materials under such conditions. Among various nano-fillers, nanoclay has demonstrated promising potential to improve the mechanical performance of rigid foams, with several experimental studies supporting its mechanical strengthening mechanisms. However, the effect of nanoclay concentration on the fracture behavior of nanocomposite foams under different loading modes, particularly Mixed-Mode I/II, remains insufficiently investigated. Gaining deeper insight into this relationship is essential for the development of nanocomposite foams tailored for safety-critical engineering applications.

This work aims to assess the fracture behaviour of rigid PUR nanocomposite foams reinforced with varying nanoclay contents (0, 1, 2, and 3 wt%) under Mixed-Mode I/II loading conditions for the first time. By applying standardized asymmetric specimen geometries and consistent test protocols, the study evaluates the influence of nanoclay content on critical mechanical metrics such as ultimate tensile strength, fracture load, and fracture toughness. This integrated approach provides a more realistic assessment of structural performance and offers essential guidance for the design of durable nanocomposite foams in advanced engineering applications.

2- Materials, Specimens, and Procedures

This section provides a comprehensive explanation of the procedures followed for the fabrication of rigid PUR nanocomposite foam specimens, including both dumbbell-shaped samples for tensile testing and disc-shaped specimens with pre-existing cracks for fracture testing. The manufacturing steps, preparation method, and geometrical specifications of the test specimens are described in detail. Additionally, the methodologies used to conduct the uniaxial tensile tests and the fracture tests under Mixed-Mode I/II loading conditions are outlined systematically. These procedures were carefully designed to ensure repeatability, reliability, and consistency with standard testing.

2-1- Materials and sample preparation

To prepare rigid PUR nanocomposite foams, isocyanate was thoroughly mixed with 1, 2 and 3 wt.% of nanoclay. To ensure uniform dispersion of nanoparticles in the base material, an ultrasonic stirrer made by Behin Tamin Ahura Company was used. The mixed material of isocyanate and nanoclay was poured into the beaker and placed in the ultrasonic mixer for 30 min. To prevent overheating of the device, the beaker was put in a bowl of cold water and set the device to turn off for 2 min after every 10 min of operation. After complete mixing of nanoclay into the isocyanate, polyol was added to the mixture and mixed for 5 s with a mechanical stirrer. It should be noted that the Instructions for making PUR nanocomposites were extracted from the datasheet of raw material manufacturing Company.

Fig. 1 illustrates how the beaker was placed inside the ultrasonic mixer.

Fig. 1: The ultrasonic setup utilized for dispersion of nanoparticles into the base material.

The mixed material was then promptly poured into two distinct molds: a dumbbell-shaped mold for preparing the uniaxial tensile samples (According to ISO 527-2), and tubular molds for the preparation of disc-shaped fracture specimens. For final curing of the samples, the molds were heated in an oven at 120 ˚C for 20 min. Finally, the foam was cut into the predefined shapes and dimensions, as will be elaborated in the upcoming subsections.

2-2- Mechanical testing

To characterize the mechanical behavior of rigid PUR nanocomposite foam, uniaxial tensile testing was performed using a Santam STM-250 universal testing machine. The tests were conducted with a crosshead displacement rate of 2 mm/min on dumbbell-shaped specimens, following ISO 527-2 standard. The shape and dimensions of the test specimens are illustrated in Fig. 2.

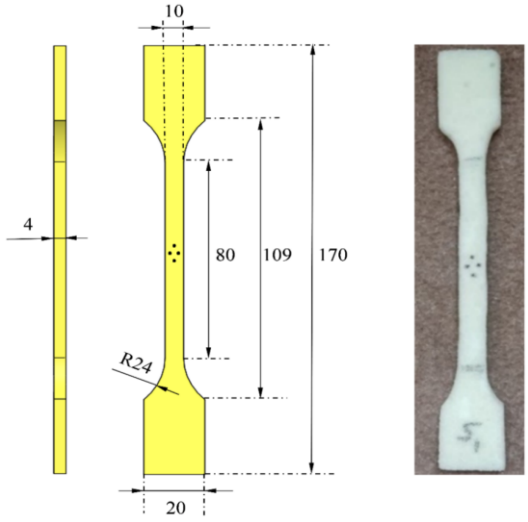

Fig. 2: Geometry and dimensions of the dumbbell-shaped sample (dimensions are in mm).

On the other hand, to evaluate the fracture toughness of the rigid PUR nanocomposite foams under different conditions, Asymmetric Edge Notch Disc Bend (AENDB) specimens were employed. These samples are specifically designed to enable measurement of both Mode-I (K_I) and Mode-II (K_{II}) fracture toughness values under Mixed-Mode loading conditions. The AENDB specimen was fabricated with a radius of R=34 mm and a uniform thickness of T=25 mm. A sharp pre-crack, a=10 mm in depth, was introduced into the specimens using a fine razor blade. The overall geometry of the AENDB specimens, along with the loading configuration used in the experiments, are presented schematically in Fig. 3.

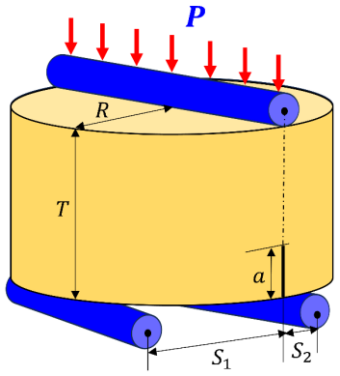

Fig. 3: The AENDB specimen used for Mixed-Mode I/II fracture tests.

For the fracture tests, the prepared AENDB specimens were carefully mounted in a three-point bending fixture, as depicted in Fig. 4. The tests were carried out at room temperature and under a constant loading rate of 2 mm/min. Throughout the experiments, the roller located on the right side of the fixture was fixed at a constant distance of S_1 =30.6 mm from the initial crack plane. Moreover, to induce various Mixed-Mode loading conditions, the position of the left support was systematically adjusted by altering the distance S_2 as indicated in Figs. 3 and 4. This setup enabled controlled investigation of fracture behavior under various combinations of Mode-I and Mode-II loading.

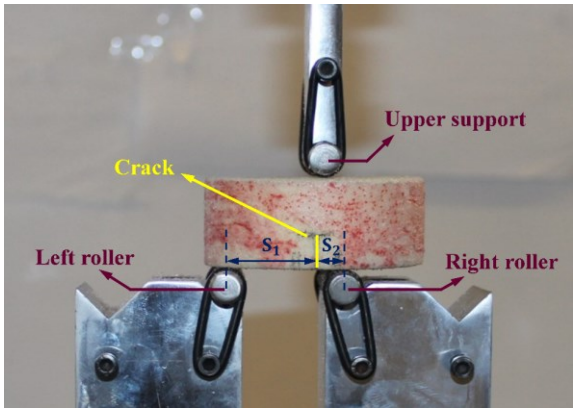

Fig. 4: Three-point bending test setup utilized for the fracture experiments in Mixed-Mode I/II.

Table 1 provides the loading configurations required for conducting fracture tests on rigid PUR nanocomposite foam under various Mixed-Mode I/II conditions. Specifically, it lists the values S_2/R ratio that corresponding to the left support distance S_2. This ratio quantifies the relative contributions of Mode-I and Mode-II in the applied loading. It is important to note that S_2/R varies from 0.9 (which represents a pure Mode-I) to 0.079 (which corresponds to pure Mode-II loading conditions). Intermediate values between 0.9 and 0.079 describe Mixed-Mode loading states.

Table 1: Loading parameters utilized for the fracture testing under Mixed-Mode I/II conditions.

$S_1(mm)$	30.6	30.6	30.6	30.6	30.6
$S_2\ (mm)$	2.7	4.1	5.4	8	30.6
S_2/R	0.079	0.121	0.159	0.235	0.9

To precisely determine the loading modes, finite element models of the specimens were created. Varying the second support position (i.e., the value of S_2) and evaluating the stress intensity factor values allowed identification of the locations where pure Mode-I and Mode-II occur.

Specifically, when S_1=S_2=30.6 mm, K_{II} approaches zero and pure Mode-I occurs. Conversely, the results of FEM revealed that positioning the second support at S_2=2.7 mm maximizes K_{II} while K_I remains zero, indicating pure Mode-II.

3- Finite Element Simulation

To accurately determine the Mixed-Mode fracture toughness values, numerical analysis was performed using Finite Element Modeling (FEM) in Abaqus software. The geometry of the AENDB specimen used in the simulation was identical to that of the experiment, consisting of a disc with a radius of 34 mm, a thickness of 25 mm, and a pre-existing crack measuring 10 mm in length. All other boundary and loading conditions, including the positions of the support rollers, were set according to the specifications listed in Table 1. To replicate realistic conditions and closely match the experimental setup, a finite element model was developed, including the AENDB specimen, one upper support, and two lower supports. Moreover, to represent the mechanical behavior of the nanocomposite specimen in the finite element model, the equivalent material properties concept was used. This methodology has been adopted in various studies for simulating the mechanical behavior of nanocomposite samples [12, 15, 31, 32]. The supports, which are actually made of high-strength steel alloy (CK45), are significantly stiffer than the foam specimen and therefore were modeled as rigid bodies. The specimen, on the other hand, was modeled as a deformable body. Moreover, a surface-to-surface contact interaction was defined between the support surfaces and the specimen to accurately simulate the physical contact behavior. The coefficient of friction between the specimen and the supports was chosen to be 0.2 [33, 34]. To apply the appropriate boundary conditions, all degrees of freedom of the lower supports were fully constrained. In addition, all degrees of freedom of the upper support were restricted except in the direction of the applied load (i.e., the Y-direction illustrated in Fig. 5) The load applied on the upper support was modeled as a uniformly distributed downward force, introduced via a reference point to ensure proper load transfer.

On the other hand, for meshing the geometry of the AENDB specimen, second-order three-dimensional continuum elements with full integration method (named as C3D20 in Abaqus) were utilized. Special attention was given to mesh refinement around the crack tip region. Fig. 5 shows the meshing of a typical AENDB sample, highlighting the finer mesh elements employed around the crack tip.

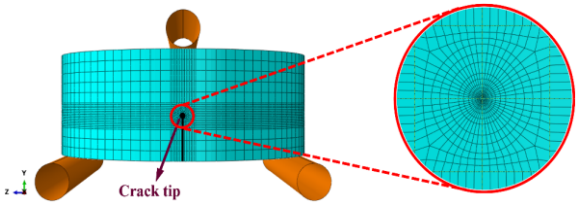

Fig. 5: A close-up view of the elements around the crack tip.

Following a mesh sensitivity analysis, the element sizes near the crack tip were selected to ensure sufficient resolution to ensure accurate computation of the stress intensity factors. Fig. 6 presents the results of the mesh sensitivity analysis for a typical sample, showing the variation of fracture toughness in pure Mode-I with the number of elements. The fracture toughness is equivalent to the stress intensity factor calculated when the critical load from the experimental test is applied in the finite element model. According to Fig. 6, employing about 40,000 elements in the complete model offers the best trade-off between accuracy and computational efficiency.

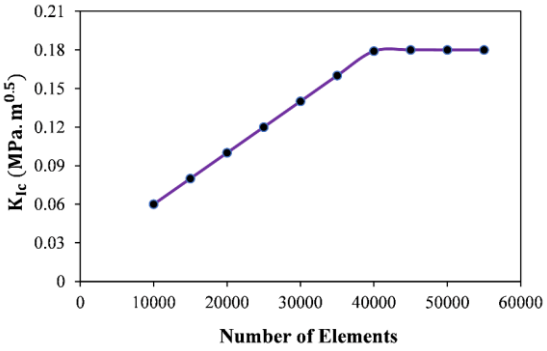

Fig. 6: The mesh sensitivity analysis: variation of K_{Ic} versus number of elements.

It should be noted that due to the complex geometry and the lack of an analytical relationship, finite element analysis was used to calculate the stress intensity factors and fracture toughness.

4- Results and discussion

In this section, the experimental results obtained from both the tensile and fracture tests conducted on rigid PUR nanocomposite foam specimens are presented and discussed.

4-1- Experimental results of tensile loading

The experimental results of the uniaxial tensile tests on rigid PUR nanocomposite foams containing 1, 2, and 3 wt% of nanoclay are first examined in this section. For a straightforward comparison of mechanical performance, each diagram presented below includes the curve of the neat foam alongside the nanocomposite ones. Fig. 7 presents the Load–Displacement curves for four dumbbell-shaped specimens containing 0, 1, 2, and 3 wt% of nanoclay. Moreover, Table 2 summarizes the mechanical properties of the rigid PUR neat and nanocomposite foams with nanoclay contents of 1, 2, and 3 wt%.

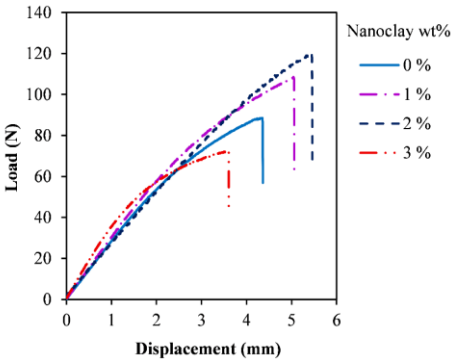

Fig. 7: Load-displacement diagram for dumbbell-shaped specimens containing 0, 1, 2, and 3 wt% of nanoclay.

Table 2: Mechanical properties of rigid PUR dumbbell-shaped neat and nanocomposite foams with 0, 1, 2, and 3 wt% of nanoclay.

Nanoclay (wt%)	$\sigma_{u,t}$ (MPa)	Critical load, F_c (N)	Critical displacement, δ_F (mm)
0 (Neat)	2.21	88.5	4.4
1	2.71	108.5	5.1
2	2.99	119.4	5.5
3	1.82	72.6	3.6

As observed from Fig. 7 and Table 2, the addition of 1 and 2 wt% of nanoclay enhances the strength of the rigid PUR foam compared to the neat sample. However, incorporating 3 wt% of nanoclay results in a reduction in tensile strength relative to the neat foam. Furthermore, it is evident that the sample containing 2 wt% of nanoclay exhibits the best mechanical performance, indicating that this concentration provides the most favorable reinforcement effect.

To better illustrate the effect of nanoclay on mechanical properties, Table 3 lists the percentage increase/decrease in the mechanical properties of each nanocomposite sample relative to the neat foam.
As can be deduced from Table 3, the specimen with 2 wt% of nanoclay displays the highest improvement in tensile strength properties, with approximately 35% increase in strength and maximum force, and about 25% enhancement in fracture displacement. In contrast, the specimen containing 3 wt% of nanoclay shows a significant reduction, with around 18% decrease in both strength and fracture displacement.

This decline can be attributed to the agglomeration of nanoparticles at higher concentrations, which leads to stress concentration points and deteriorates the overall mechanical integrity of the foam.

Table 3: Variation in mechanical properties at each wt% of nanoclay compared to the neat foam (%).

Nanoclay (wt%)	$\sigma_{u,t}$	Critical load, F_c	Critical displacement, δ_F
1	22.6	22.6	15.9
2	35.3	34.9	25.0
3	- 17.6	- 18.0	- 18.2

4-2- Experimental results of fracture tests under pure Mode-I and pure Mode-II

This section presents the experimental results obtained from three-point bending fracture tests conducted on rigid PUR nanocomposite foams containing 1, 2, and 3 wt% of nanoclay under Mixed-Mode I/II loading conditions. To determine the optimal nanoclay concentration for enhancing fracture resistance in our tested nanocomposite foams, fracture tests were performed under pure Mode-I and pure Mode-II loading conditions for all nanoclay contents. Accordingly, the load–displacement curves for the neat and nanocomposite foam specimens tested under these two loading modes were obtained and the results are illustrated in Fig. 8. It should be noted that the term *Displacement* in this diagram represents the vertical displacement of the upper punch during the bending test, until the complete fracture of the samples.

As illustrated in Fig. 8, the addition of 1 wt% and 2 wt% of nanoclay enhances the mechanical properties of the nanocomposite foams, yielding higher fracture loads compared to the neat foam. Conversely, incorporating 3 wt% of nanoclay negatively impacts the foam's strength, leading to a noticeable reduction in fracture load These findings indicate that, consistent with the uniaxial tensile behavior, 2 wt% nanoclay offers the most effective enhancement in the fracture resistance of rigid PUR foams. In addition, incorporating 2 wt% nanoclay results in a 32% enhancement in fracture load under pure Mode-I and a 22% increase under Mode-II loading, compared to the neat foam. On the other hand, the addition of 3 wt% nanoclay leads to a 35% and 20% reduction in fracture load under Mode-I and Mode-II, respectively.
To justify this finding, it should be emphasized that the agglomeration of nanoparticles occurs when they cluster together due to high surface energy and van der Waals forces, resulting in reduced surface area and non-uniform dispersion within the host matrix. This phenomenon negatively impacts the properties of nanocomposites, such as mechanical strength and thermal stability, by hindering effective load transfer and interaction between the nanoparticles and the matrix. In the case of nanoclay agglomeration in rigid PUR foam, the issue becomes even more pronounced due to the highly reactive and rapidly expanding nature of the foam system. Nanoclay particles tend to cluster during the foaming process because of poor compatibility with the polyol and isocyanate components and insufficient exfoliation. Thus, these agglomerates act as stress concentrators, leading to reduced cell uniformity, irregular pore structures, and weaker interfacial bonding between the nanoclay and the polymer matrix. Consequently, the mechanical and thermal insulation properties of the foam may deteriorate rather than improve.

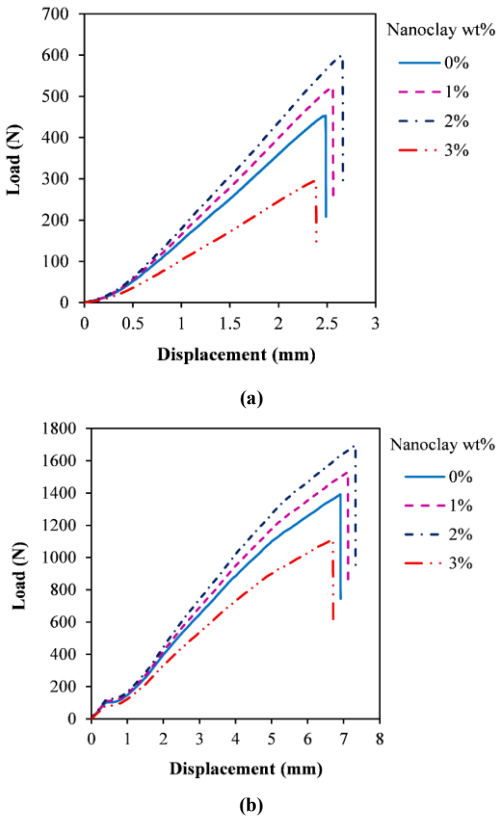

Fig. 8: Load–displacement curves of fracture tests for the neat and nanocomposite foams under (a) pure Mode-I and (b) pure Mode-II.

To enable further comparison of the nanoclay's effect on foam fracture behavior, finite element simulations were carried out for all specimens based on the established procedure, and fracture toughness values were determined for each tested sample. The relevant fracture toughness values under pure Mode-I and Mode-II loading conditions are summarized in Table 4.

Table 4: Fracture toughness of rigid PUR neat and nanocomposite foams with 0, 1, 2, and 3 wt% nanoclay.

Nanoclay (wt%)	K_{Ic} (MPa. $m^{0.5}$)	K_{IIc} (MPa. $m^{0.5}$)
0 (Neat)	0.18	0.14
1	0.19	0.15
2	0.2	0.16
3	0.15	0.11

According to the results shown in Fig. 8 and Table 4, adding 1 and 2 wt% of nanoclay improves both the strength and fracture toughness of the rigid PUR foam compared to the unreinforced sample. In contrast, incorporating 3 wt% of nanoclay leads to a decrease in these properties relative to the neat foam. Among all tested formulations, the foam containing 2 wt% of nanoclay demonstrated the greatest fracture resistance, indicating that this concentration provides the most efficient reinforcement.
To further clarify the influence of nanoclay on fracture toughness, Table 5 provides the percentage change in fracture toughness under pure Mode-I and pure Mode-II loading conditions for each nanocomposite sample compared to the neat foam.

Table 5: Variation in fracture toughness at each wt% nanoclay compared to the neat foam (%).

Nanoclay (wt%)	K_{Ic} (MPa. $m^{0.5}$)	K_{IIc} (MPa. $m^{0.5}$)
1	5.5	7.1
2	11.1	14.3
3	- 16.7	- 21.4

As shown in Table 5, the foam with 2 wt% nanoclay demonstrates the greatest enhancement in fracture toughness, while the 3 wt% nanoclay sample experiences a notable reduction. This decrease is likely due to nanoparticle agglomeration at higher loadings, which can create localized stress concentrations and impair the foam's overall fracture performance.

4-3- Experimental results of fracture tests under Mixed-Mode I/II

Since the sample with 2 wt% of nanoclay showed the best results in the uniaxial tension as well as in pure Mode-I and pure Mode-II fracture tests, the mixed-mode I/II fracture experiments were exclusively carried out on this formulation to reduce laboratory costs, and the results are compared with the neat foam sample. The load–displacement curves obtained from the three-point bending tests for the Mixed-Mode I/II fracture states are illustrated in Fig. 9.

To enable a direct comparison, Table 6 reports the experimental fracture loads of the neat foam and the 2 wt% of nanoclay nanocomposite foam under Mixed-Mode I/II conditions, along with the differences between their values.

Table 6: The experimental fracture load of the neat foam and the nanocomposite foam with 2 wt% of nanoclay under Mixed-Mode I/II loading conditions (N).

wt% nanoclay	S_2/R				
	0.079	0.121	0.159	0.235	0.9
0 (Neat)	1392.2	1292.2	1140.6	1002.6	453.3
2	1698.5	1495.8	1425.8	1253.3	594.8
Variation (%)	22.0	15.8	25.0	25.0	32.0

According to the data in Table 6, the 2 wt% nanoclay nanocomposite foam shows a remarkable enhancement in fracture load relative to the neat foam, with improvements ranging from 15.8% ($S_2/R = 0.121$) to 32% ($S_2/R = 0.9$). This finding demonstrates the effectiveness of nanoclay at an optimal concentration in improving the fracture resistance of rigid PUR foams under mixed-mode loading.

5- Conclusions

This study has clearly demonstrated the reinforcing effectiveness of nanoclay in rigid PUR foams. Both experimental and FEM results confirmed that incorporating 2 wt% of nanoclay significantly enhances tensile strength and fracture resistance under complex Mixed-Mode I/II loading conditions. However, increasing the nanoclay content to 3 wt% led to performance deterioration due to nanoparticle agglomeration, which induced stress concentration zones and compromised the foam's structural integrity. Mixed-Mode I/II fracture tests revealed that the addition of nanoclay increased the fracture load by up to 32%, particularly under Mode-I dominant conditions. Moreover, the fracture toughness of the sample containing 2 wt% nanoclay increased by approximately 11.1% and 14.3% in pure Mode-I and pure Mode-II, respectively, compared to the neat foam. In contrast, the sample with 3 wt% of nanoclay exhibited a reduction in fracture toughness of about 16.7% in pure Mode-I and 21.4% in pure Mode-II.

Overall, this study emphasizes the importance of optimizing nanoclay concentration and ensuring uniform particle dispersion during processing. It also confirms that rigid PUR nanocomposite foams reinforced with nanoclay hold strong potential for high-performance applications in automotive, aerospace, and construction industries, where lightweight materials with superior durability and fracture resistance are essential.

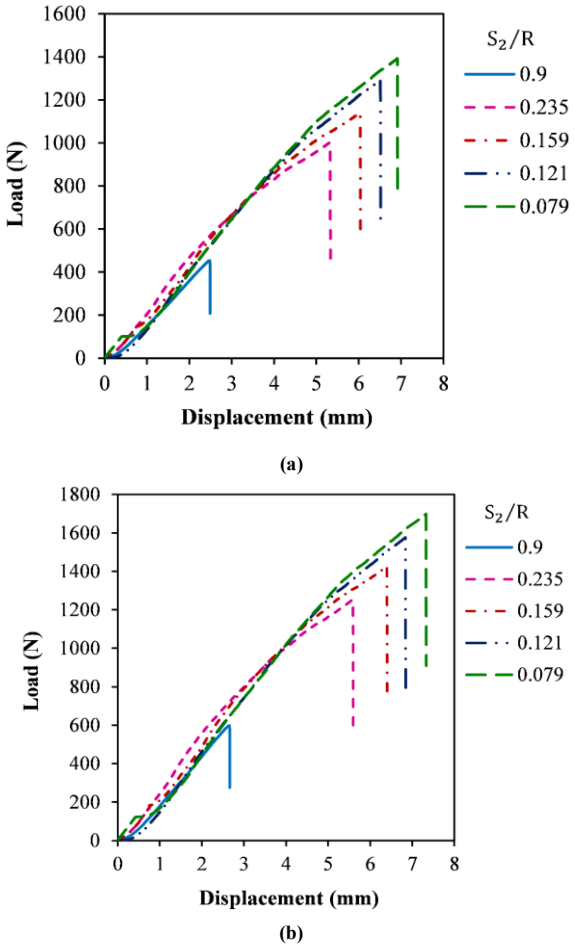

Fig. 9: Load–displacement curves under Mixed-Mode I/II loading conditions for the rigid PUR foam containing (a) neat and (b) 2 wt% of nanoclay.

Ethics Approval

The scientific content of this article is the result of the authors' research and has not been published in any Iranian or international journal.

Conflict of Interest

The authors affirm that there is no conflict of interest regarding the publication of this article, as all data reported are derived from their own research activities.

References

[1] S. S. Ray and M. Okamoto, "Polymer/layered silicate nanocomposites: a review from preparation to processing," Progress in polymer science, vol. 28, no. 11, pp. 1539-1641, 2003.DOI: 10.1016/j.progpolymsci.2003.08.002.

[2] G. Harikrishnan, T. U. Patro, and D. Khakhar, "Polyurethane foam− clay nanocomposites: nanoclays as cell openers," Industrial & Engineering Chemistry Research, vol. 45, no. 21, pp. 7126-7134, 2006. DOI: 10.1021/ie0600994.

[3] P. Saraeian, H. Tavakoli, and A. Ghassemi, "Production of polystyrene-nanoclay nanocomposite foam and effect of nanoclay particles on foam cell size," Journal of Composite Materials, vol. 47, no. 18, pp. 2211-2217, 2013. DOI 10.1177/0021998312454906.

[4] B. Saboori and M. R. Ayatollahi, "CNT influence on fracture toughness of a polymer-based nanocomposite under the out-of-

plane shear in comparison with pure tensile loading conditions," (in eng), Modares Mechanical Engineering, vol. 16, no. 10, pp. 441-447, 2017. [Online]. Available: http://mme.modares.ac.ir/article-15-5980-en.html.

[5] M. Kamali Moghaddam and M. Tahani, "Study the effect of environment temperature on mechanical and fracture behavior of carbon nanotubes," (in eng), Modares Mechanical Engineering, vol. 17, no. 3, pp. 87-92, 2017. [Online]. Available: http://mme.modares.ac.ir/article-15-8685-en.html.

[6] C. Zeng, N. Hossieny, C. Zhang, B. Wang, and S. M. Walsh, "Morphology and tensile properties of PMMA carbon nanotubes nanocomposites and nanocomposites foams," Composites science and technology, vol. 82, pp. 29-37, 2013. DOI: 10.1016/j.compscitech.2013.03.024.

[7] M. Colloca, N. Gupta, and M. Porfiri, "Tensile properties of carbon nanofiber reinforced multiscale syntactic foams," Composites Part B: Engineering, vol. 44, no. 1, pp. 584-591, 2013. DOI: 10.1016/j.compositesb.2012.02.030.

[8] M. Santiago-Calvo, J. Tirado-Mediavilla, J. L. Ruiz-Herrero, M. Á. Rodríguez-Pérez, and F. Villafane, "The effects of functional nanofillers on the reaction kinetics, microstructure, thermal and mechanical properties of water blown rigid polyurethane foams," Polymer, vol. 150, pp. 138-149, 2018. DOI: 10.1016/j.polymer.2018.07.029.

[9] K. Cherednichenko, D. Kopitsyn, E. Smirnov, N. Nikolaev, and R. Fakhrullin, "Fireproof nanocomposite polyurethane foams: a review," Polymers, vol. 15, no. 10, p. 2314, 2023. DOI: 10.3390/polym15102314.

[10] R. Babaei, M. M. Touiserkani, M. Khanchoupan, and A. Afradi, "Numerical Simulation of the Effect of Conventional and Hybrid Nanofluids on the Cooling Performance of Automobile Radiator," Journal of Science and Technology in Mechanical Engineering, vol. 3, no. 2, pp. 137-151, 2025. DOI: 10.22034/STME.2025.504084.1103.

[11] H. Movahhedi Aleni, G. H. Lighat, M. h. Pol, and A. Afrouzian, "An experimental investigation on mode-II interlaminar fracture toughness of nanosilica modified glass/epoxy fiber-reinforced laminates," (in eng), Modares Mechanical Engineering, vol. 15, no. 3, pp. 283-290, 2015. [Online]. Available: http://mme.modares.ac.ir/article-15-4924-en.html.

[12] M. Heydari-Meybodi, S. Saber-Samandari, and M. Sadighi, "A new approach for prediction of elastic modulus of polymer/nanoclay composites by considering interfacial debonding: experimental and numerical investigations," Composites Science and Technology, vol. 117, pp. 379-385, 2015. DOI: 10.1016/j.compscitech.2015.07.014.

[13] m. Kerman Saravi, M. H. Pol, and M. H. Sattari, "Experimental investigation of the influence of adding nanotubes on Mode I interlaminar fracture toughness of laminated composites," (in eng), Modares Mechanical Engineering, vol. 16, no. 3, pp. 193-201, 2016. [Online]. Available: http://mme.modares.ac.ir/article-15-9931-en.html.

[14] F. Guo, S. Aryana, Y. Han, and Y. Jiao, "A review of the synthesis and applications of polymer–nanoclay composites," Applied Sciences, vol. 8, no. 9, p. 1696, 2018. DOI: 10.3390/app8091696.

[15] A. Ghasemi and M. Gharehbash, "Ductile Fracture Analysis of Notched Epoxy Nanocomposites Reinforced with Graphene Oxide Nanoparticles Using the Equivalent Material Concept," (in eng), Modares Mechanical Engineering, vol. 24, no. 4, pp. 215-223, 2024. DOI: 10.48311/mme.24.4.215.

[16] X. Cao, L. J. Lee, T. Widya, and C. Macosko, "Polyurethane/clay nanocomposites foams: processing, structure and properties," Polymer, vol. 46, no. 3, pp. 775-783, 2005. DOI 10.1016/j.polymer.2004.11.028.

[17] M. Saha, M. E. Kabir, and S. Jeelani, "Enhancement in thermal and mechanical properties of polyurethane foam infused with nanoparticles," Material Science and Engineering: A, vol. 479, no. 1-2, pp. 213-222, 2008. DOI :10.1016/j.msea.2007.06.060.

[18] E. S. Ali and S. Ahmad, "Bionanocomposite hybrid polyurethane foam reinforced with empty fruit bunch and nanoclay," Composites Part B: Engineering, vol. 43, no. 7, pp. 2813-2816, 2012. DOI: 10.1016/j.compositesb.2012.04.043.

[19] A. Kausar, I. Rafique, and B. Muhammad, "Aerospace application of polymer nanocomposite with carbon nanotube, graphite, graphene oxide, and nanoclay," Polymer-Plastics Technology and Engineering, vol. 56, no. 13, pp. 1438-1456, 2017. DOI: 10.1080/03602559.2016.1276594.

[20] N. V. Gama, A. Ferreira, and A. Barros-Timmons, "Polyurethane foams: Past, present, and future," Materials, vol. 11, no. 10, p. 1841, 2018. DOI: 10.3390/ma11101841.

[21] H. Somarathna, S. Raman, D. Mohotti, A. Mutalib, and K. Badri, "The use of polyurethane for structural and infrastructural engineering applications: A state-of-the-art review," Construction and Building Materials, vol. 190, pp. 995-1014, 2018. DOI: 10.1016/j.conbuildmat.2018.09.166.

[22] M. M. Touiserkani and M. Heydari Meybodi, "On the use of J-integral criterion for fracture assessment of cracked rigid polyurethane foam loaded in mixed mode I/II and I/III," Journal of Solid and Fluid Mechanics, vol. 14, no. 3, pp. 141-151, 2024. DOI: 10.22044/jsfm.2024.14305.3847.

[23] R. H. Alasfar, S. Ahzi, N. Barth, V. Kochkodan, M. Khraisheh, and M. Koç, "A review on the modeling of the elastic modulus and yield stress of polymers and polymer nanocomposites: Effect of temperature, loading rate and porosity," Polymers, vol. 14, no. 3, p. 360, 2022. DOI: 10.3390/polym14030360.

[24] R. K. Ramakrishnan and N. S. Sumitha, "Nanoclay-reinforced polymers," in *Nanoclay-based sustainable materials*: Elsevier, 2024, pp. 91-114. DOI: 10.1016/B978-0-443-13390-9.00006-0.

[25] I. Javni, W. Zhang, V. Karajkov, Z. Petrovic, and V. Divjakovic, "Effect of nano-and micro-silica fillers on polyurethane foam properties," Journal of Cellular Plastics, vol. 38, no. 3, pp. 229-239, 2002. DOI: 10.1177/0021955X02038003139.

[26] Z. Sajadian, S. M. Zebarjad, and M. Bonyani, "Thermal and mechanical properties of honeycomb sandwich panel of polyurethane nanocomposite reinforced with nanoclay," Journal of Polymer Research, vol. 31, no. 9, p. 284, 2024. DOI: 10.1007/s10965-024-04130-0.

[27] S. Chuayjuljit, A. Maungchareon, and O. Saravari, "Preparation and properties of palm oil-based rigid polyurethane nanocomposite foams," Journal of Reinforced Plastics and Composites, vol. 29, no. 2, pp. 218-225, 2010. DOI: 10.1177/0731684408096949.

[28] S. Kim, M. Lee, H. Kim, H. Park, H. Jeong, K. Yoon, and B. Kim, "Nanoclay reinforced rigid polyurethane foams," Journal of Applied Polymer Science, vol. 117, no. 4, pp. 1992-1997, 2010. DOI: 10.1002/app.32116.

[29] R. R. Maharsia and H. D. Jerro, "Enhancing tensile strength and toughness in syntactic foams through nanoclay reinforcement," Material Science and Engineering: A, vol. 454, pp. 416-422, 2007. DOI: 10.1016/j.msea.2006.11.121.

[30] Q. Zhang, X. Lin, W. Chen, H. Zhang, and D. Han, "Modification of rigid polyurethane foams with the addition of nano-SiO2 or lignocellulosic biomass," Polymers, vol. 12, no. 1, p. 107, 2020. DOI: 10.3390/polym12010107.

[31] H. Zarei, M. Fallah, H. Bisadi, A. Daneshmehr, and G. Minak, "Multiple impact response of temperature-dependent carbon nanotube-reinforced composite (CNTRC) plates with general boundary conditions," Composites Part B: Engineering, vol. 113, pp. 206-217, 2017. DOI: 10.1016/j.compositesb.2017.01.021.

[32] M. H. Meybodi, S. Saber-Samandari, M. Sadighi, and M. R. Bagheri, "Low-velocity impact response of a nanocomposite

beam using an analytical model," Latin American Journal of Solids and Structures, vol. 12, no. 2, pp. 333-354, 2015. DOI: 10.1590/1679-78251346.

[33] M. M. Touiserkani and M. Heydari-Meybodi, "Out-of-plane fracture in plane strain conditions: A novel criterion with analytical and experimental evaluation in thick PUR foam," Mechanics of Materials, p. 105499, 2025. DOI: 10.1016/j.mechmat.2025.105499.

[34] S. Yao, Z. Chen, P. Xu, Z. Li, and Z. Zhao, "Experimental and numerical study on the energy absorption of polyurethane foam-filled metal/composite hybrid structures," Metals, vol. 11, no. 1, p. 118, 2021. DOI: 10.3390/met11010118.